Geophysica (2023), 58 (1), 47–75

Heatwave projections for Finland at different levels of global warming derived from CMIP6 simulations

Kimmo Ruosteenoja[1,*] *and Kirsti Jylhä*[1]

[1]Finnish Meteorological Institute, P. O. Box 503, FI-00101 Helsinki, Finland
[*]Corresponding mail address: kimmo.ruosteenoja@fmi.fi

(Submitted: 2023-08-23; Accepted: 2023-10-26)

Abstract

Even in the cool climate of Finland, severe heatwaves occur sporadically, having multiple implications on public health, forestry, fishery, agriculture, and reindeer husbandry, for instance. This study assesses the occurrence and severity of ≥ 3 *-day heatwaves in Finland at the* 0.5 °C*,* 1.0 °C*,* 1.5 °C*, and* 2.0 °C *global warming levels above pre-industrial conditions, utilising bias-corrected daily-mean temperature data from* 60 *runs performed with* 25 *global climate models. The severity of a heatwave is measured by the heatwave extremity index, consisting of the sum of exceedances above a fixed threshold of daily mean temperature. Three alternative threshold temperatures,* 20 °C*,* 24 °C *and* 28 °C*, are considered.*

A shift from the 0.5 °C *to* 2.0 °C *global warming level is projected to result in an increase in the mean annual number of heatwave days above* 20 °C *from* 1 *to* 5 *in central Lapland and from* 5 *to* 20 *in south-eastern Finland. Concurrently, the annual sum of the extremity index becomes* 4 *to* 10 *-fold. The higher the threshold temperature, the larger is the growth in relative terms. At the* 2.0 °C *global warming level, heatwaves above* 20 °C *are experienced in southern Finland nearly every year and in the majority of northern Lapland approximately every second year. Apart from Lapland, heatwaves occurring once in* 10 *(*100*) years at the* 0.5 °C *warming level will then have annual probabilities of* 50 % *(*> 10 %*).*

Even between the 1.5 °C *and* 2.0 °C *global warming levels, projected changes in heatwave characteristics are substantial, especially for the most severe heatwaves. For example, in southern and central Finland, a heatwave with an annual probability of* 12 % *to* 13 % *at the* 1.5 °C *warming level is projected to substantially increase in likelihood under the* 2.0 °C *warming level, up to* 19 % *to* 21 %*.*

The paper includes a literature review on potential impacts of the intensifying heatwaves.

Keywords: climate change; global climate models; bias correction; global warming levels; heatwave extremity index; return levels

1 Introduction

In Finland, global warming is projected to lead to a substantial increase in the summer temperatures; for example, if the medium-level Shared Socioeconomical Path SSP2-4.5 greenhouse gas scenario (*O'Neill et al.*, 2016) were realised, the mean temperatures of June–August would rise by 3.3 °C (with an uncertainty interval of 1.2 °C to 5.3 °C) from the period 1981–2010 to 2070–2099 (*Ruosteenoja and Jylhä*, 2021). It is evident that, in tandem with the projected warming, heatwaves are becoming increasingly severe. The purpose of the present work is to investigate future changes in heatwave characteristics by utilising bias-corrected data from global climate model simulations.

According to observations, the number and heat sum of hot days have already increased statistically significantly in southern Finland (*Aalto et al.*, 2023; *Rantanen et al.*, 2023). *Seneviratne et al.* (2021) and *Wang et al.* (2022) likewise report recent increases in the frequency and intensity of heatwaves in multiple areas of the globe, including northern Europe. According to *Otto et al.* (2012), as a consequence of the observed warming, probabilities for the occurrence of a heat wave as extreme as that experienced in Russia in 2010 were approximately three times as large as it would have been in the climate of the 1960s.

In the future, projected changes in multiple heatwave indices tend to be larger in southern than northern Europe, but the responses are far from negligible in the north as well (*Cardell et al.*, 2020; *Ruosteenoja and Jylhä*, 2023). For Finland, *Ruosteenoja et al.* (2013) assessed that the number of hot days (with the daily mean temperature above 20 °C) would become 3–4 -fold by the end of this century (period 2070–2099), compared with the baseline period covering the last three decades of the 20$^{\text{th}}$ century. However, that analysis examined an obsolete greenhouse gas scenario that was stronger than what is currently regarded as realistic. In *Kim et al.* (2018), in the 21$^{\text{st}}$ century on average, the number of hot days in Finland was projected to be approximately double as large as in the 20$^{\text{th}}$ century.

The present work constitutes a sequel to our previous research that examined $\geq$3-day future heatwaves over the entire European continent (*Ruosteenoja and Jylhä*, 2023, hereafter referred to RJ23). Nevertheless, even though the model data are the same, all the findings presented here are completely fresh. This is so because, unlike in RJ23, we now use fixed rather than percentage-based threshold temperatures for a hot day, i.e., the daily mean temperatures of 20, 24 and 28 °C. The same thresholds have been employed in many previous Finnish heatwave studies that analysed data from antecedent climate model generations (e.g., *Kim et al.*, 2018; *Ruosteenoja et al.*, 2013). A fixed threshold temperature is a rational choice when examining heatwave characteristics in a limited area within which the climate does not vary too much, like Finland, Czechia (*Kyselý*, 2010), or Poland and Germany (*Tomczyk and Bednorz*, 2019). In contrast, in our previous study covering the entire Europe (RJ23), we had to use percentile-based threshold temperatures, because it was not possible to find a common threshold value that would be appropriate both for the cool Finnish and hot Portuguese climate, for instance.

In this work, heatwaves are examined in modelled climates that correspond to the global mean temperature increases of 0.5, 1.0, 1.5, and 2.0 °C relative to the pre-industrial level. The two lowest warming levels represent global temperatures that prevailed in the late 20$^{\text{th}}$ century and in the 2010s (RJ23), while the two highest ones are equivalent to the more and less stringent targets of the Paris Agreement on Climate Change signed in 2015. This kind of approach is very generally used in the current scientific literature (*Seneviratne et al.*, 2021), since it aids to eliminate distractions caused by the models that simulate unrealistically strong or weak global warming (e.g., *Hausfather et al.*, 2022). Accordingly, the influence of inter-model divergence in the global warming sensitivity is removed, leaving only the differences in how the models allocate warming to the different

seasons and regions of the globe.

The paper is structured as follows. Section 2 describes the model output data used and processing of the data. Also, the heatwave indices are defined, with the key indicator being the heatwave extremity index or the sum of exceedances above the threshold temperature; this is a quantity analogous to the heat accumulation of the growing season. Section 3 reports projected long-term mean changes in the heatwave indices, while the anticipated occurrence of the most extreme discrete heat periods is discussed in Section 4. The discussion Section 5 specifically compares differences in the heatwave characteristics between the 1.5 °C and 2 °C global warming levels and considers some potential sources of uncertainty in the analysis. As well, a literature review on potential societal and environmental impacts of the intensifying heatwaves is offered. The paper is finalised by concluding remarks in Section 6.

2 Model data and analyses

In this section, only the key points of the analysis methods are described, so that one is able to interpret the findings presented in the subsequent sections. For further technical details, the reader is referred to Section 2 of RJ23.

2.1 Bias-adjusted model data

Heatwave projections were derived from 25 global climate models (GCMs) participating in Phase 6 of the Coupled Model Intercomparison Project (CMIP6, *Eyring et al.*, 2016), fulfilling the following conditions: (i) temperature data had to be available at the daily-mean level and (ii) the model was regarded as at least reasonably capable to be used for studying future climate changes in Finland in our previous studies (RJ23; *Ruosteenoja*, 2021; *Ruosteenoja and Jylhä*, 2021). Considering the parallel runs, 60 GCM runs were utilised (Table 1 of RJ23). Data from historical GCM runs were explored by 2014 and those corresponding to the SSP2-4.5 greenhouse-gas scenario thereafter.

Before the analyses, a bias correction was employed for the GCM output data. The procedure (method M7; see *Räisänen and Räty*, 2013 and *Ruosteenoja et al.*, 2016) forces the simulated baseline-period means and temporal standard deviations of the daily mean temperatures for each calendar month to match with the observational data (version 23 of the E-OBS analysis, *Haylock et al.*, 2008). The resulting correction coefficients were then used to adjust the simulated future temperatures. An important advantage of the method is that GCM-simulated changes in the mean temperature from the baseline period to the future are not distorted. Simultaneously, the spatial resolution of the temperature data is improved tremendously (RJ23, Figs. 1–2). The same bias correction method was used by *Kim et al.* (2018) in their heatwave projection study.

Thanks to the bias correction, in all the adjusted model output datasets the global mean temperature of the period 1977–1996 is virtually precisely 0.5 °C warmer than in the pre-industrial era. This 20-year period will be used as a reference for the future projections.

To explore the higher global warming levels, the point of time when the 20-year running global mean temperature has increased by 1.0, 1.5, or 2.0 °C relative to the pre-industrial era was searched from the bias-corrected GCM data. The time point diverges among the various GCMs; for example, the two-degree warming level is reached, depending on the model, between 2026 and 2078 (RJ23, Table 1). The multi-model medians of the crossing years are 2009 for the 1.0 °C, 2027 for the 1.5 °C and 2044 for the 2.0 °C warming. In the study, the indices describing heatwave characteristics were calculated for the 20-year period surrounding the crossing year. For example, if the year of crossing is 2045, the period studied is 2035–2054. In principle, the search for the periods representing the different warming levels was carried out in a similar way as in the recent IPCC report (*Seneviratne et al.*, 2021, Cross-Chapter Box 11.1), however, taking into account the impact of the bias correction.

According to section 11.2.4 of *Seneviratne et al.* (2021), simulated changes in temperature-related variables at a certain level of global warming have proved to be approximately similar regardless of the greenhouse gas scenario that has led to this warming level. Consequently, it is adequate to analyse data from the responses to a single greenhouse-gas scenario (SSP2-4.5). Admittedly, using this forcing scenario involves the limitation that 2.5 °C or higher global warming levels could not be explored since some GCMs never reach so strong warming under SSP2-4.5.

2.2 Heatwave indices and analyses

As stated in the introduction, a hot day is defined here by considering the daily mean temperature rather than the daily maximum. This approach has been followed in many previous studies (e.g., *Kim et al.*, 2018; *Kollanus et al.*, 2021; *Ouzeau et al.*, 2016; *Sambou et al.*, 2021), even though the maximum temperatures have been examined quite widely as well (e.g., *Lhotka et al.*, 2018; *Tomczyk and Bednorz*, 2019). The daily mean temperature takes into account both the hotness of the day and high temperatures prevailing in the night. The daytime heat is not that detrimental if the coolness of the night periodically provides relief (*Zhu et al.*, 2022, and references therein). For example, low night-time temperatures act to cool buildings. Moreover, it is often possible to schedule commuting between home and workplace as well as other outdoor activities to the morning and evening hours, thus avoiding the impact of the highest temperatures that generally prevail in early afternoon. In addition, daily maximum temperature data were not available from all the models, and in some models the data proved to be unusable (*Ruosteenoja*, 2021). Accordingly, the use of daily-mean temperatures enlarges the model ensemble analysed and improves the robustness of the findings.

Correspondingly, a heatwave episode is a spell during which the threshold temperature (20 °C, 24 °C or 28 °C) is exceeded for at least 3 consecutive days. The 3-day minimum length for a heatwave is commonly used in the literature (e.g., *Cardell et al.*, 2020; *Kim et al.*, 2018; *Lhotka et al.*, 2018; *Sambou et al.*, 2021; *Tomczyk and Bednorz*, 2019). The heatwave period is defined to continue until the daily mean temperature falls below the threshold for at least two days. Hence, one day in between does not yet terminate

the heatwave. The same definition was used in *Baldwin et al.* (2019), for instance. To give an illustrative example, if the threshold temperature is first exceeded for 3 days, then fallen below in one day but again exceeded for 2 days, the total length of the heatwave event is 6 days. In RJ23, we explored alternative options, allowing either 0 or 2 break days within the heatwave. Nonetheless, the related sensitivity experiments showed that the impact of break days on the projected relative changes of the heatwave indices was minor (Section 5.1 and Fig. 13 of RJ23).

The 3-day minimum length of a heatwave can be justified by that the full realization of damages, such as health issues, overheating of buildings and wilting of vegetation, requires several hot days in a row. For example, *Sohail et al.* (2020) state that it is several-day heatwaves rather than single hot days that act to increase morbidity. On the other hand, a single cooler day does not yet allow the human bodies to recover (*Baldwin et al.*, 2019) or does not sufficiently cool the buildings (*Ramamurthy et al.*, 2017), if the heatwave again continues thereafter.

The main indices used here to characterise heatwave severity are the length of the heatwave period and the heatwave extremity index EX. For EX, the following definition is used:

$$\mathrm{EX} = \sum_{t=t_\mathrm{o}}^{t_\mathrm{e}} \max\left(T_\mathrm{day}(t) - T_0, 0\right) \ , \tag{2.1}$$

where T_day is the daily mean temperature and T_0 the threshold temperature. t_o and t_e stand for the onset and termination dates of the event. Accordingly, EX consists of the sum of exceedings above the threshold temperature across the heatwave period, that is, EX depends on both the length and warmth of the heat period. Indices identical or analogous to EX have been widely used in the literature, albeit the names used for the index diverge (for citations, see Section 2.3 of RJ23).

In the present work, the period with the highest EX is regarded as the most severe heatwave of the year. In order to facilitate interpretation of the values of EX, Fig. 2.1 shows the annual maximum observational EX above 20 °C for six summers with significant heatwaves in Finland. In a hot summer, in southern Finland the maximum EX typically falls on between 20 and 60 °C days, being mainly at most ∼20 °C days in the north.

However, in 1972 an exceptionally intense period of heat was experienced in northern Finland (Fig. 2.1a). Near Ivalo, EX even amounted up to > 60 °C days. In eastern Lapland, the heat stressed reindeers severely, and they started collapse during the reindeer separation, so that the animals had to be released from the enclosures (*Turunen et al.*, 2016). Considering the entire Finland, the hot summer of 1972 caused approximately 800 extra human deaths (*Näyhä*, 2005).

Even in southern Finland, the limit of 60 °C days has not been exceeded in wide areas until the years 2010 and 2018. In the record-breaking summer of 2010, in south-eastern Finland the maximum EX was locally higher than 80, on the Karelian Isthmus (former territory of Finland) even > 140 °C days (Fig. 2.1d). This was just the summer when central Russia experienced nearly an unimaginably intense heatwave episode; for more information, see *Barriopedro et al.* (2011) and Fig. 3c of RJ23.

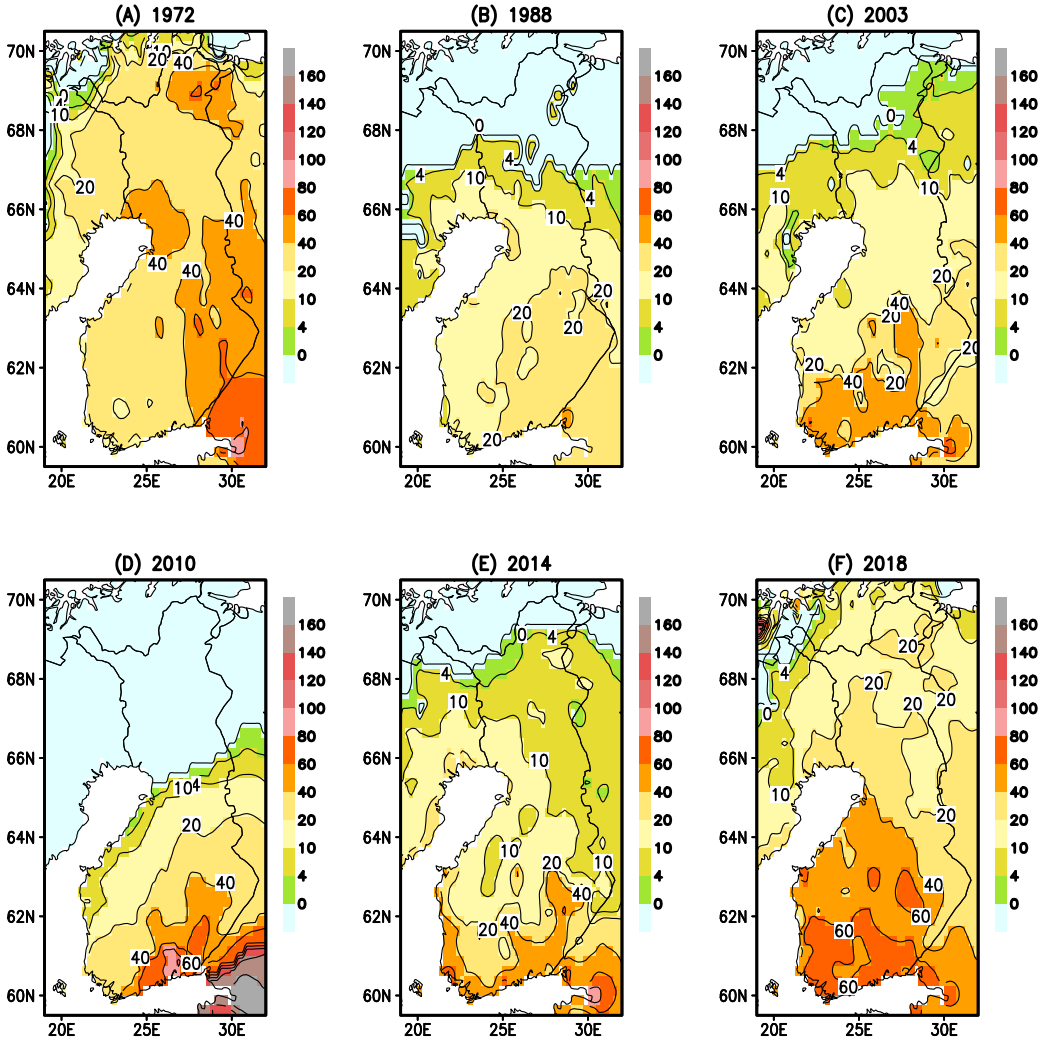

Fig. 2.1: Heatwave extremity indices (unit °C days) derived from the E-OBS-analyses for six severe annual maximum heat spells that occurred in Finland in (a) 1972, (b) 1988, (c) 2003, (d) 2010, (e) 2014 and (f) 2018. The threshold temperature is 20 °C.

In examining the long-term mean changes, we shall show temporal averages of the total annual number of heatwave days and the sum of EX over all the heatwave periods of the year. Thereafter, we look at the annual probabilities for the occurrence of heatwave events, separately for the three threshold temperatures. For studying the occurrence of extreme heat episodes, we first concatenated bias-adjusted data of all the model runs to create 1,200-year long time series (60 runs times 20 a/run) to represent each of the four global warming levels. Such a large sample provides statistically reliable estimates for the various heatwave indicators. Then, for each 'year' of the time series, we searched for the heatwave with the largest EX. This maximum EX dataset was used to determine various recurrence levels of EX (e.g., for the 10 and 100-year return periods) in the climate of the baseline period (0.5 °C global warming level). Finally, it was investigated at what likelihood those return levels were exceeded during a year at the 1.0 °C, 1.5 °C, and 2.0 °C warming levels.

Owing to the bias correction, in the baseline-period climate temporal variations in the 1,200-a time series purely reflect interannual variability in weather conditions. At the 1.0 °C to 2.0 °C warming levels, fluctuations are induced by both interannual variability and the divergent warming of the Finnish warm-season climate in the various GCMs. Nevertheless, the entire sample of 1200 years represent a similar global warming level.

3 Long-term mean changes

To infer time-mean changes in the extremity index and the count of heatwave days, we first calculated 20-year temporal means of the indices for each model run, then averaged these over the parallel runs of the GCM and finally calculated multi-model means from the parallel-run averages. All 25 GCMs were weighted equally.

The mean annual number of heatwave days at the four global warming levels is shown in Fig. 3.1. In the baseline climate (0.5 °C global warming level), there is on average less than one heatwave day per summer in the northernmost Finland and more than 5 days in the southeast (Fig. 3.1a). The geographical distribution is qualitatively similar to that reported in Table 7 of *Ruosteenoja et al.* (2013), with more abundantly hot days in southern Finland and the Eastern and Central Finland lake district than in Kainuu, Ostrobothnia, and Lapland. At the 2.0 °C warming level, the number of heatwave days is projected to increase to 1–5 in northern Lapland and to more than 20 in the southeast (Fig. 3.1d). In an absolute sense, the increase is largest in the areas where the count of heatwave days is greatest in the baseline climate, but it is vice-versa when looking at the relative increase (Fig. 3.2).

The choice of the reference period affects the projected change substantially, especially on the relative increase. When comparing the 2.0 °C global warming level to the 0.5 °C level, the count of heatwave days approximately quadruples in southern and eastern Finland and becomes up to 10-fold in north-western Lapland (Fig. 3.2c). When using the 1.0 °C warming level representing the very recent past as a reference, the corresponding ratio varies between $\leq$2 and 4 (Fig. 3.2d).

Figure 3.3 gives an idea of how the total annual number of heatwave days increases

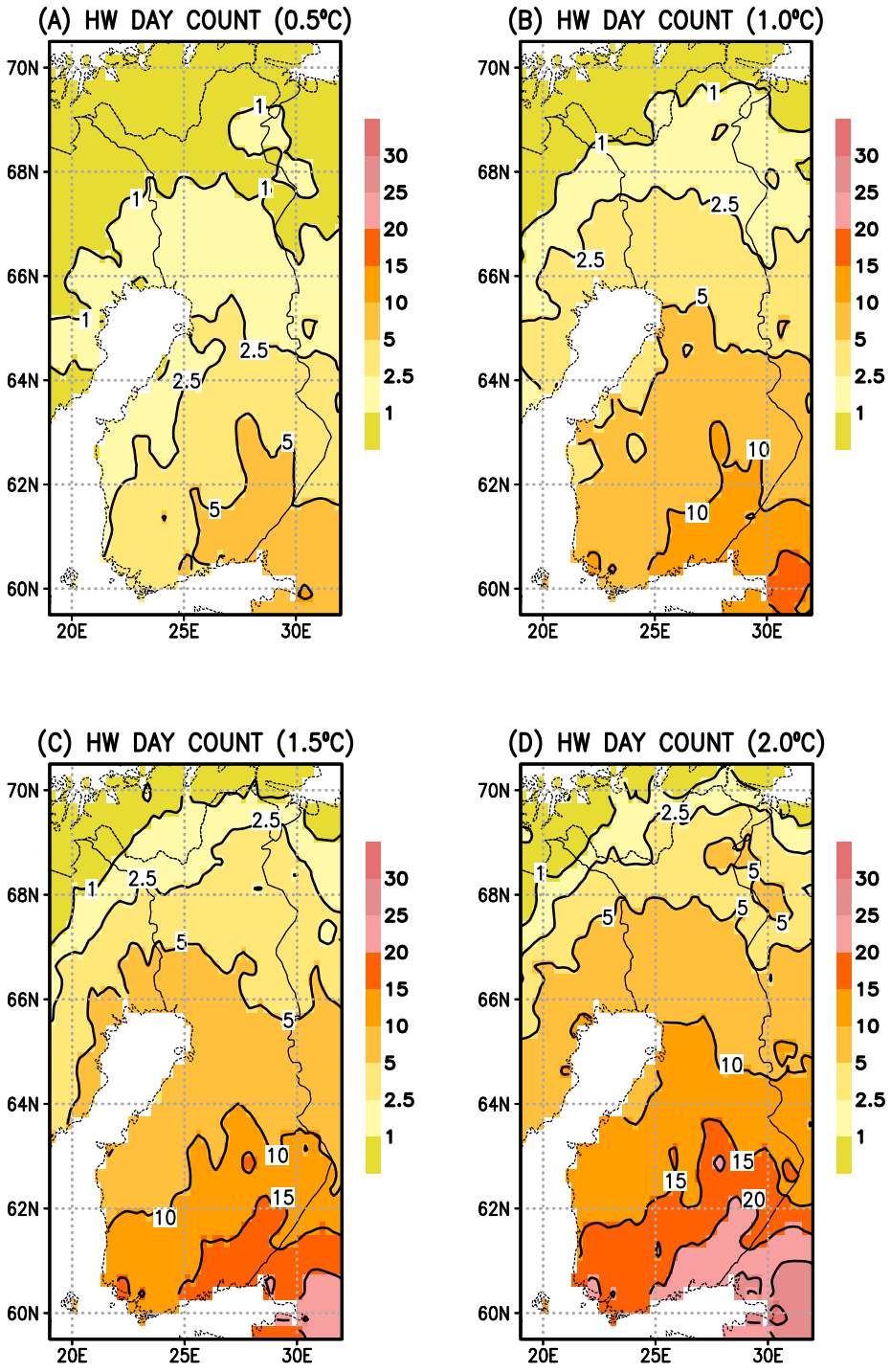

Fig. 3.1: Mean annual number of heatwave days above the 20 °C threshold temperature (multi-model 20-year averages) in Finland and its adjacent areas under the global warming levels of (a) 0.5 °C, (b) 1.0 °C, (c) 1.5 °C and (d) 2.0 °C.

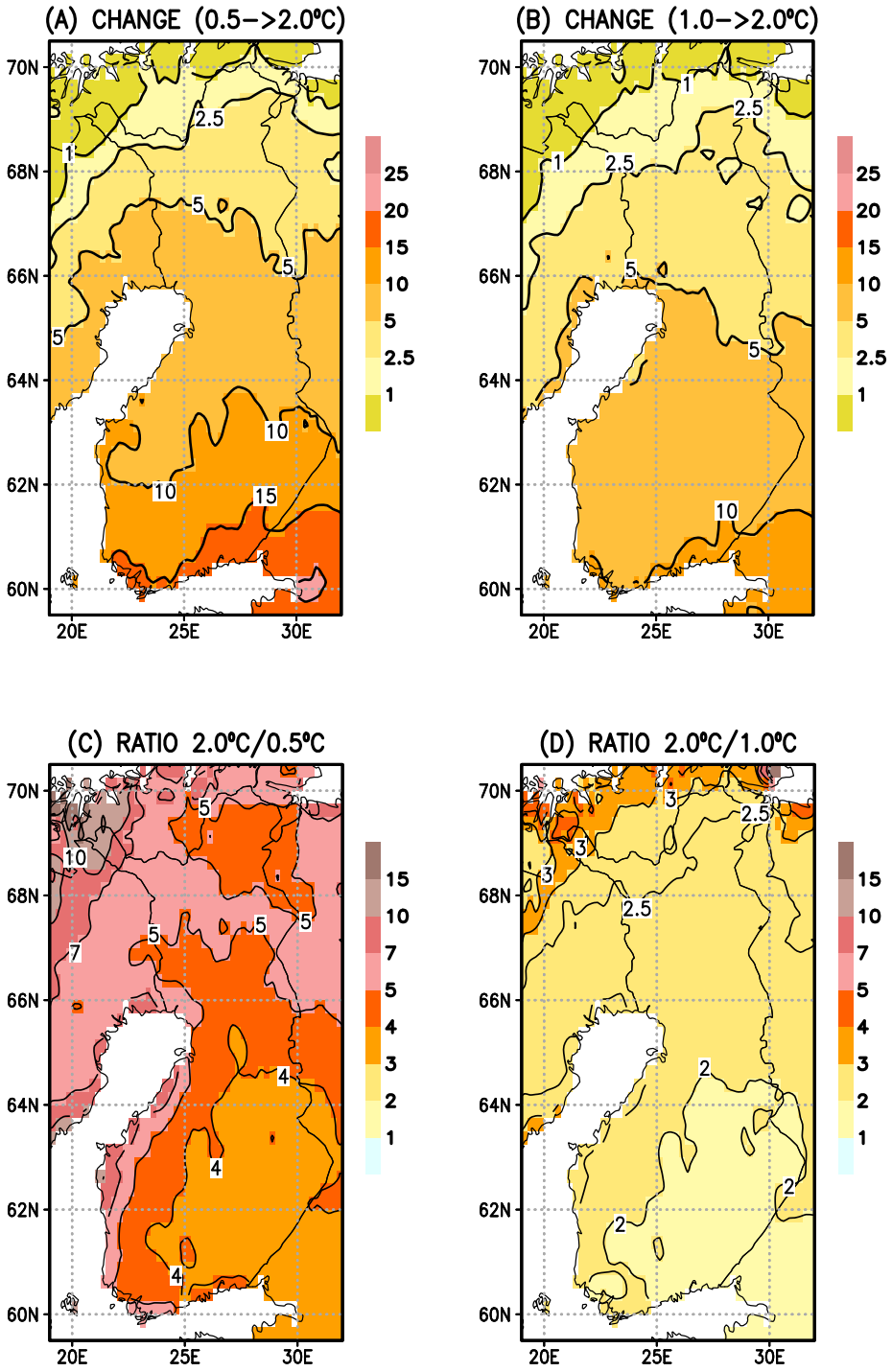

Fig. 3.2: Projected changes in the average number of heatwave days from the (a) 0.5 °C and (b) 1.0 °C global warming level to the 2.0 °C level and the corresponding ratios of the heatwave-day number at the 2.0 °C level to that at the (c) 0.5 °C and (d) 1.0 °C level. For definitions, see the caption of Fig. 3.1.

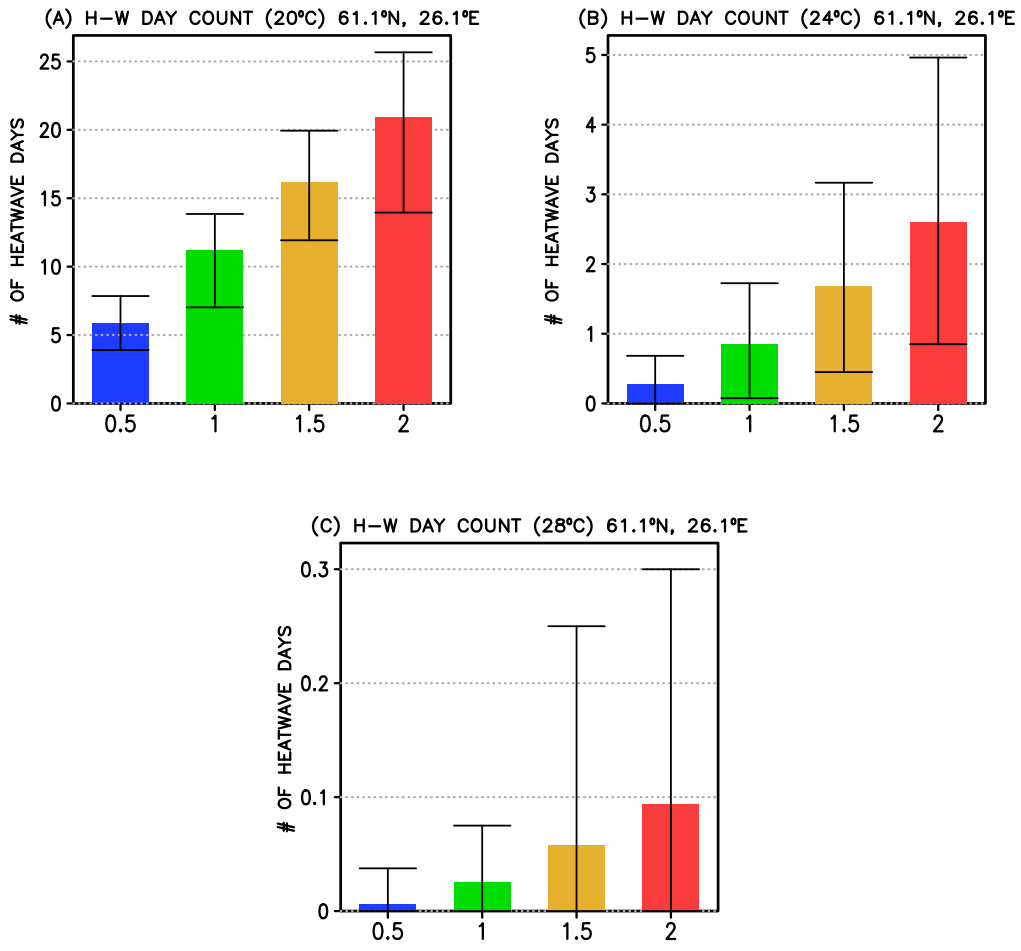

Fig. 3.3: The 20-year mean total annual number of heatwave days under the global warming levels of 0.5 °C (blue), 1.0 °C (green), 1.5 °C (yellow) and 2.0 °C (red) at 61.125°N, 26.125°E (close to Heinola) using the threshold temperature of (a) 20 °C, (b) 24 °C and (c) 28 °C. Coloured bars depict multi-model means and error bars the interval between the second-lowest and second-highest GCM, nominally defining the 6 to 94 % uncertainty interval.

at a single position in southern Finland. The average number of heatwave days is presented for all three threshold temperatures and considering both the multi-model means and uncertainty intervals reflecting inter-model scatter. As expected, heatwave days monotonically become more common as a function of global warming. The absolute increase is the largest for the 20 °C but the relative increase for the 28 °C threshold temperature (Fig. 3.3). For the lowest threshold temperature, the increase is nearly linearly proportional to global warming, but for the higher thresholds, the increase tends to accelerate as the global warming proceeds.

Furthermore, Fig. 3.3 reveals that there is considerable divergence among the projections produced by the various GCMs, although the global mean temperature increase between periods is identical. In relative terms, the differences are largest when examining the highest threshold temperature. Such very intense heatwaves are infrequent, and their occurrence is thus strongly affected by stochastic factors. Reasons behind the inter-model scatter are discussed in more detail in Section 5.2.

The time-mean annual sum of the heatwave extremity index increases in northern Lapland from less than 2 °C days under the 0.5 °C warming level to 5 °C to 10 °C days at the 2.0 °C level and in the southeast, from about 10 to 50 °C days (Fig. 3.4). So, for this measure as well, the absolute increase is largest in the areas where the baseline values are highest (Fig. 3.5a–b). Conversely, the relative increase is largest in the north, where the total annual EX becomes up to 15 or 3-fold, depending on whether the late-20$^{\text{th}}$ century or the recent past climate is used as the reference (Fig. 3.5c–d).

It is noteworthy that, in a relative sense, EX increases more rapidly than the number of heatwave days (compare Figs. 3.5c–d and 3.2c–d). This is so because EX will be enhanced not only by the lengthening but also by the higher temperatures of the heatwave periods, which act to increase temperature exceedances relative to the threshold temperature in Eq. (2.1).

To obtain a deeper insight into the projected changes of EX, Table 3.1 shows the total annual sum of EX under different warming levels at three positions, located (i) in southern Finland near the town of Heinola, (ii) in Ostrobothnia near Oulu, and (iii) in the northern Finnish Lapland near Ivalo. All three threshold temperatures and both the multi-model means and inter-model scatter are considered. In analogy to the count of heatwave days (Fig. 3.3), the total extremity index increases unambiguously as the global climate warms, in such a way that the absolute increase is smallest but the relative increase largest for the highest threshold temperatures (Table 3.1). Even so, inter-model divergence is substantial. For example, according to the lower end of the uncertainty range, at the two northernmost points there would occur no heatwaves above 24 °C or 28 °C at any of the four warming levels examined. Conversely, if the upper end of the range were realised, at the 2.0 °C level even heatwaves above the 28 °C threshold (that are unprecedented up to now) would occur at all three positions.

A somewhat peculiar finding in Table 3.1 is that the long-term mean of EX above 28 °C is larger in northern Lapland than at the Ostrobothnian point. One reason behind this finding may be that the temporal standard deviation of summer daily-mean temperatures

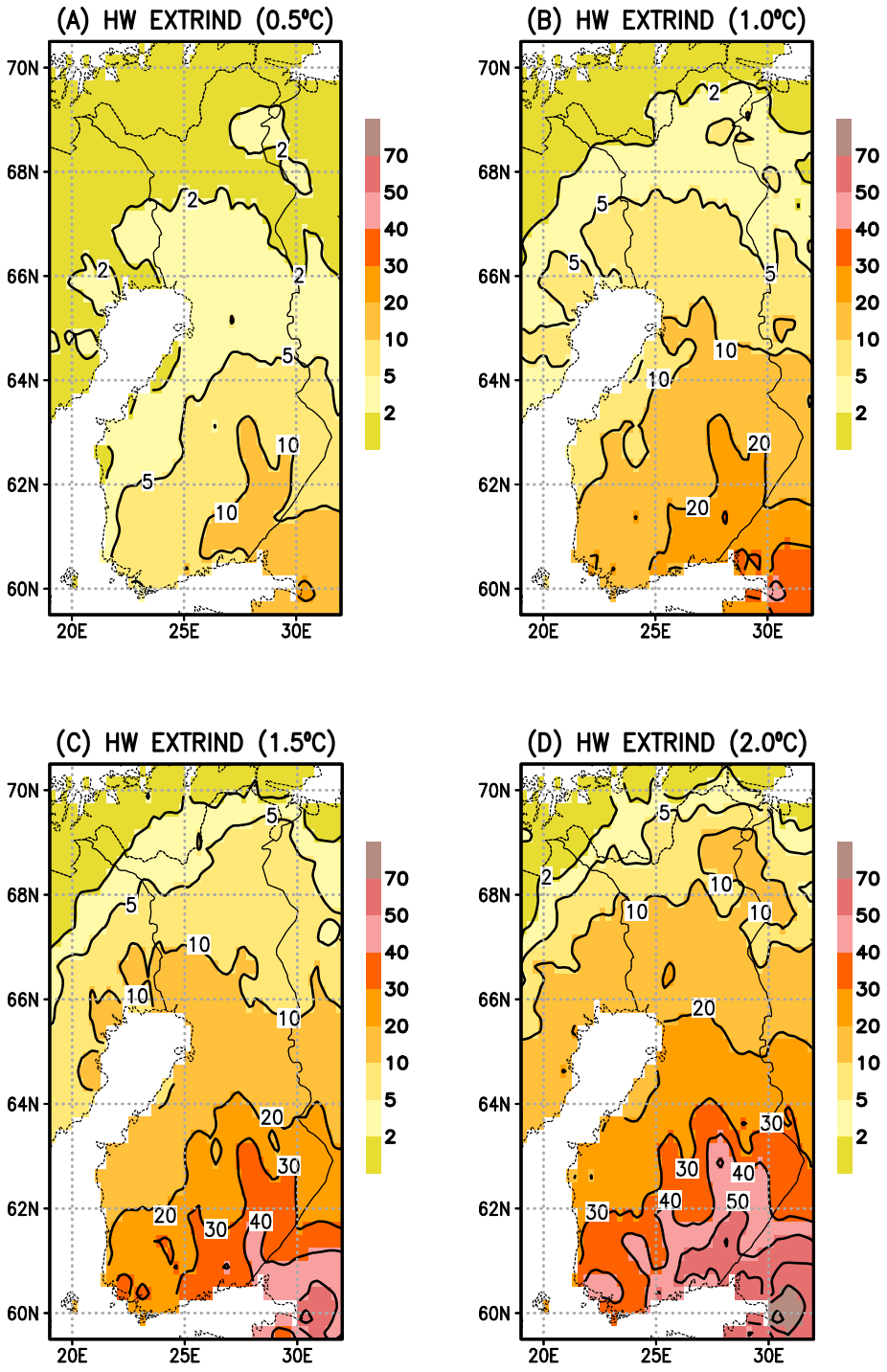

Fig. 3.4: Mean annual sum of the extremity index EX over all the heatwave spells of the year (multi-model 20-year averages; threshold temperature 20°C) under the global warming levels of (a) 0.5 °C, (b) 1.0 °C, (c) 1.5 °C and (d) 2.0 °C. Unit °C days.

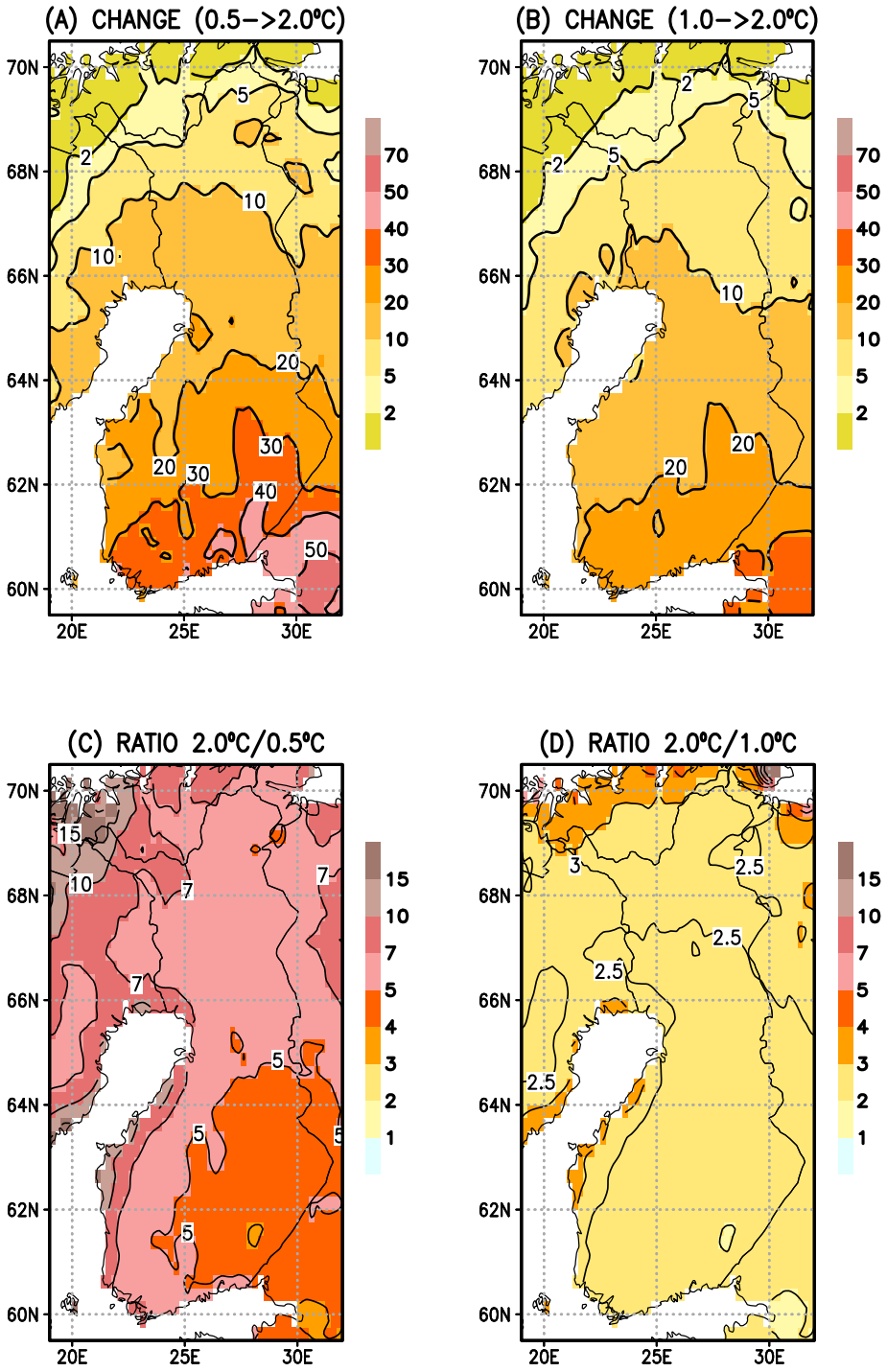

Fig. 3.5: Projected changes (in °C days) in the average total annual heatwave extremity index from the (a) 0.5 °C and (b) 1.0 °C global warming level to the 2.0 °C level and the corresponding ratios of the index at the 2.0 °C level to that at the (c) 0.5 °C and (d) 1.0 °C level. For definitions, see the caption of Fig. 3.4.

Table 3.1: Temporally averaged total annual heatwave extremity index EX (unit °C days) under four levels of global warming (0.5 °C, 1.0 °C, 1.5 °C, and 2.0 °C) at three grid points: 61.125°N, 26.125°E (southern), 65.125°N, 25.625°E (central/Ostrobothnian) and 68.625°N, 27.625°E (northern). The multi-model mean index value is given first, followed by the 6 % to 94 % uncertainty interval reflecting inter-model divergence in parentheses. The estimates are shown separately for three threshold temperatures: (a) 20 °C, (b) 24 °C, and (c) 28 °C. Unit: degree days.

(a) Threshold temperature 20 °C

Grid point	0.5 °C	1.0 °C	1.5 °C	2.0 °C
Southern	11.0 (6.8–15.7)	23.6 (13.8–33.7)	36.8 (25.8–49.1)	49.9 (35.8–68.4)
Central	4.2 (1.7– 8.7)	10.4 (5.1–15.7)	17.1 (11.4–27.9)	25.0 (14.2–38.4)
Northern	2.6 (0.9– 5.5)	5.4 (1.7–10.4)	8.9 (2.8–18.7)	13.4 (4.6–23.8)

(b) Threshold temperature 24 °C

Grid point	0.5 °C	1.0 °C	1.5 °C	2.0 °C
Southern	0.42 (0.00–1.36)	1.42 (0.08–3.51)	2.93 (0.44–6.58)	4.78 (1.00–9.31)
Central	0.07 (0.00–0.29)	0.35 (0.00–1.07)	0.76 (0.00–2.63)	1.50 (0.00–3.68)
Northern	0.10 (0.00–0.34)	0.36 (0.00–1.48)	0.74 (0.00–3.28)	1.05 (0.00–2.32)

(c) Threshold temperature 28 °C

Grid point	0.5 °C	1.0 °C	1.5 °C	2.0 °C
Southern	0.01 (0.00–0.03)	0.04 (0.00–0.12)	0.08 (0.00–0.46)	0.17 (0.00–0.59)
Central	0.00 (0.00–0.00)	0.00 (0.00–0.00)	0.00 (0.00–0.00)	0.02 (0.00–0.11)
Northern	0.00 (0.00–0.00)	0.02 (0.00–0.09)	0.03 (0.00–0.14)	0.03 (0.00–0.17)

is larger in Lapland than elsewhere in Finland (Fig. 1b of RJ23), which acts to produce occasional very high daily-mean temperatures in the bias-corrected GCM output data. A deeper examination of this topic is beyond the scope of the present study.

In RJ23, we likewise studied differences between the multi-model means and medians of both the above-discussed heatwave indices. However, as can be seen in Fig. 6 of that paper, differences between the two statistics proved to be negligible.

In interpreting Figs. 3.1–3.5 and Table 3.1, it is important to keep in mind that, according to the definition applied in the present work, the minimum length of a heatwave episode is 3 days. Consequently, for example, 0.1 very extreme heatwave days per summer on average at the 2.0 °C warming level (red column on the right in Fig. 3.3c) does not indicate that there should be approximately one day with the mean temperature above 28 °C in every tenth year. Rather, this figure refers to a 3-day extremely hot period that tends to occur, on average, once in 30 years (or a longer period even less frequently). Moreover, even if the projected EX in Table 3.1 is equal to zero, this does not rule out the potential occurrence of single very hot days that do not constitute three-day sequences. In fact, the 28 °C daily-mean temperature was exceeded in places in eastern Finland in the late July of 2010 (*Hutila*, 2010).

In addition to the intensity of heatwaves, RJ23 explored the time of year of their occurrence. In central Europe, the average mid-point date of the most intense heatwave of the year was delayed by about one week (Fig. 9 of RJ23). In northern Europe, by contrast,

changes in the timing were fairly small, 0–4 days.

4 Probabilities for the occurrence of heatwaves with different intensities

4.1 Proportion of years with heatwaves

Figure 4.1 shows probabilities for the occurrence of at least one ≥3-day heatwave in a year at the 1.0 and 2.0 °C global warming levels, separately for the three threshold temperatures. At the 1.0 °C warming level, moderately hot periods (above the 20 °C threshold temperature) occur in northern Lapland north of 67°N in 10–40 % of all summers, in south-eastern Finland in 8 summers out of 10. At the 2.0 °C warming level, the corresponding likelihoods are 20–60 % in the north and 90–95 % in the south and east, indicating that in the latter area heatwaves would be experienced nearly every year.

Severe heatwave episodes above the 24 °C threshold temperature occur in southern and eastern Finland in the simulated recent past climate (1.0 °C warming level) 1–2 times/decade but in the warmed climate (2.0 °C warming level) 2–4 times/decade (Figs. 4.1b and e). At the latter warming level, such heatwaves are experienced approximately once a decade as far as in central Lapland.

Very extreme heatwaves, i.e., the daily-mean temperatures exceeding 28 °C in ≥3 consecutive days, are very unlikely to occur in the current climate, with annual probabilities of ∼0.5 % in the southeast and virtually zero in the north (Fig. 4.1c). However, at the 2.0 °C warming level the annual probability of their occurrence would amount to more than 2 % in the south (Fig. 4.1f).

4.2 Changes in the frequency of extreme heatwaves

As stated in Section 2, we first determined the 4–100 year return levels of the strongest annual heatwave for the 0.5 °C global warming level, and these return-level values were then employed to assess probabilities for such heatwaves at higher warming levels. Owing to the large size of the sample, 1,200 modelled years, the recurrence levels could be retrieved directly from the frequency distributions. Finally, we estimated probabilities for the extremity index being higher than a fixed level, 60 °C days.

As an illustrative example, estimates of the 10- and 100-year return levels of the annual maximum EX above the 20 °C threshold temperature under the 0.5 °C warming level are shown in Fig. 4.2. As expected, the return-level values are highest in the south and southeast and smallest in the north. For example, the 100-year recurrence level ranges from about 20 °C days in northern Lapland to 60 °C days in the southeast; in elevated fell areas in the furthest north, the values are still lower. It can be seen that the very intense historical heatwave experienced in Lapland in 1972 (Fig. 2.1a) far exceeded even the 100-year return level estimate. Nevertheless, it should be recalled that the bias-correction algorithm employed in the present work does not adjust the skewness of the frequency distribution. Consequently, in the model output data, potential biases in the skewness of daily-mean temperatures may influence the occurrence of extremely high temperatures. In the south, the 100-year baseline-period return level (40–60 °C days) was not widely

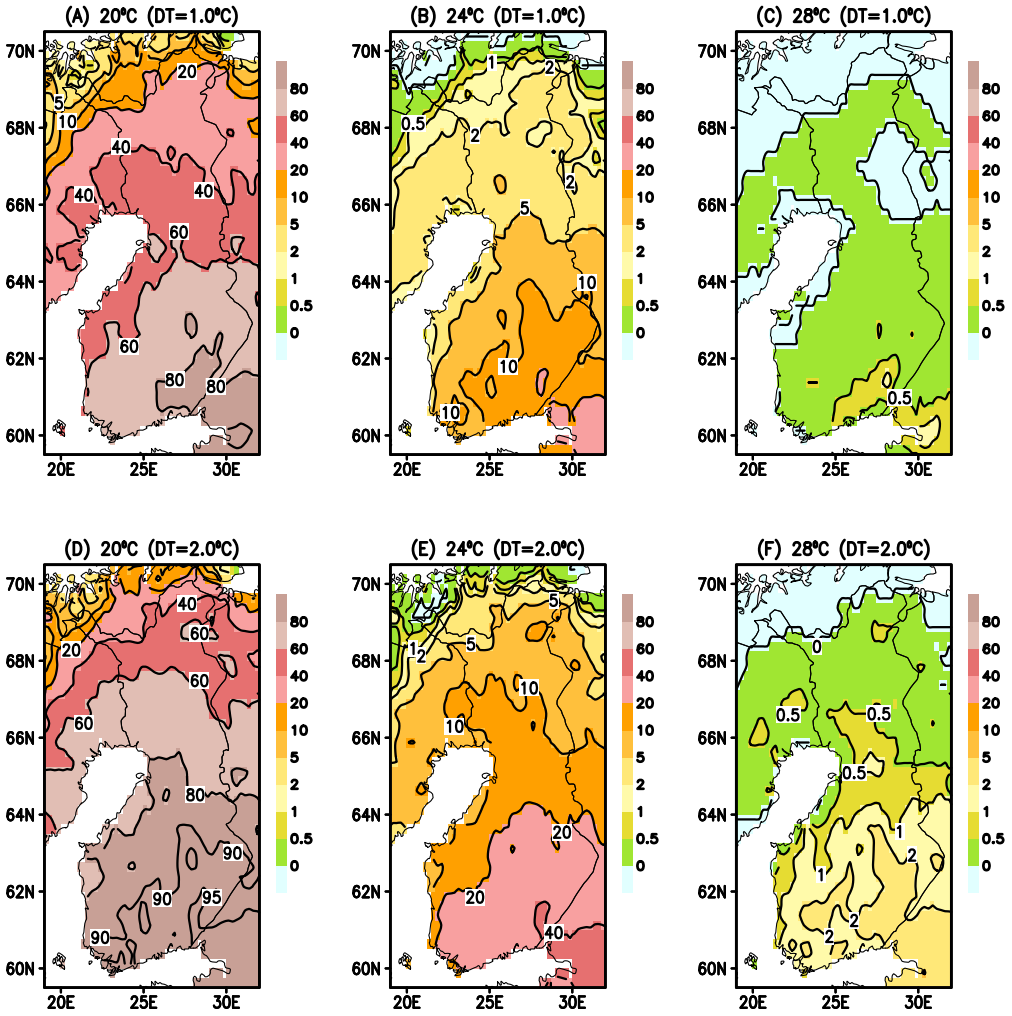

Fig. 4.1: Probabilities (in %) for the occurrence of at least a single three-day period with the daily mean temperature exceeding (a, d) 20 °C, (b, e) 24 °C and (c, f) 28 °C in a year under the (a–c) 1.0 °C and (d–f) 2.0 °C global warming levels. Probabilities have been derived from the concatenated multi-model datasets.

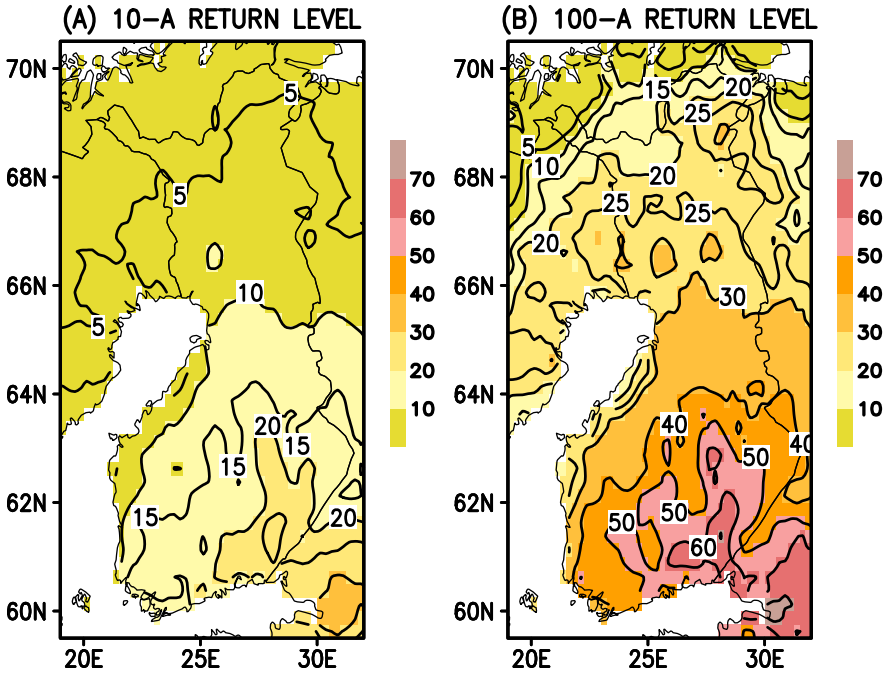

Fig. 4.2: Return levels for the extremity index of the most intense heatwave of the year (above the 20°C threshold temperature; unit °C days) under the 0.5 °C global warming level, derived from the concatenated multi-model frequency distribution: (a) 10-year and (b) 100-year return level.

exceeded until 2003, 2010, and 2018 (Figs. 2.1c, d and f), but in those years climate had already warmed considerably compared to the baseline conditions.

The occurrence of severe heatwave events at the various levels of global warming, considering the different baseline-period return levels, are shown in Fig. 4.3. The three grid points examined are the same as in Table 3.1, lying close to Heinola, Oulu, and Ivalo. In the course of global warming, the probabilities tend to increase drastically. For example, in southern Finland such a heatwave that occurs on average once in 10 years in the baseline-period climate has an annual probability of approximately 37 % at the 1.5-degree warming level and 51 % at the 2-degree level. In the region of Oulu, the probabilities are nearly the same, but in the very north somewhat lower (28 % and 40 %). Correspondingly, the annual probabilities of an historical once-in-100 year heatwave at the 2.0 °C warming level are 9–15 %.

The above-stated probabilities indicate that very rare heatwaves (e.g., with a 100-year recurrence period in the baseline climate) become, in relative terms, increasingly frequent more rapidly than the fairly common ones (e.g., with a 10 year recurrence period); this inference is consistent with the findings of *Seneviratne et al.* (2021). Moreover, the probabilities of occurrence tend to increase more pronouncedly in the south than north. An analogous spatial distribution is apparent at the entire European level as well (Fig. 12 of RJ23), and potential reasons for the phenomenon are discussed in Section 6.1 of that

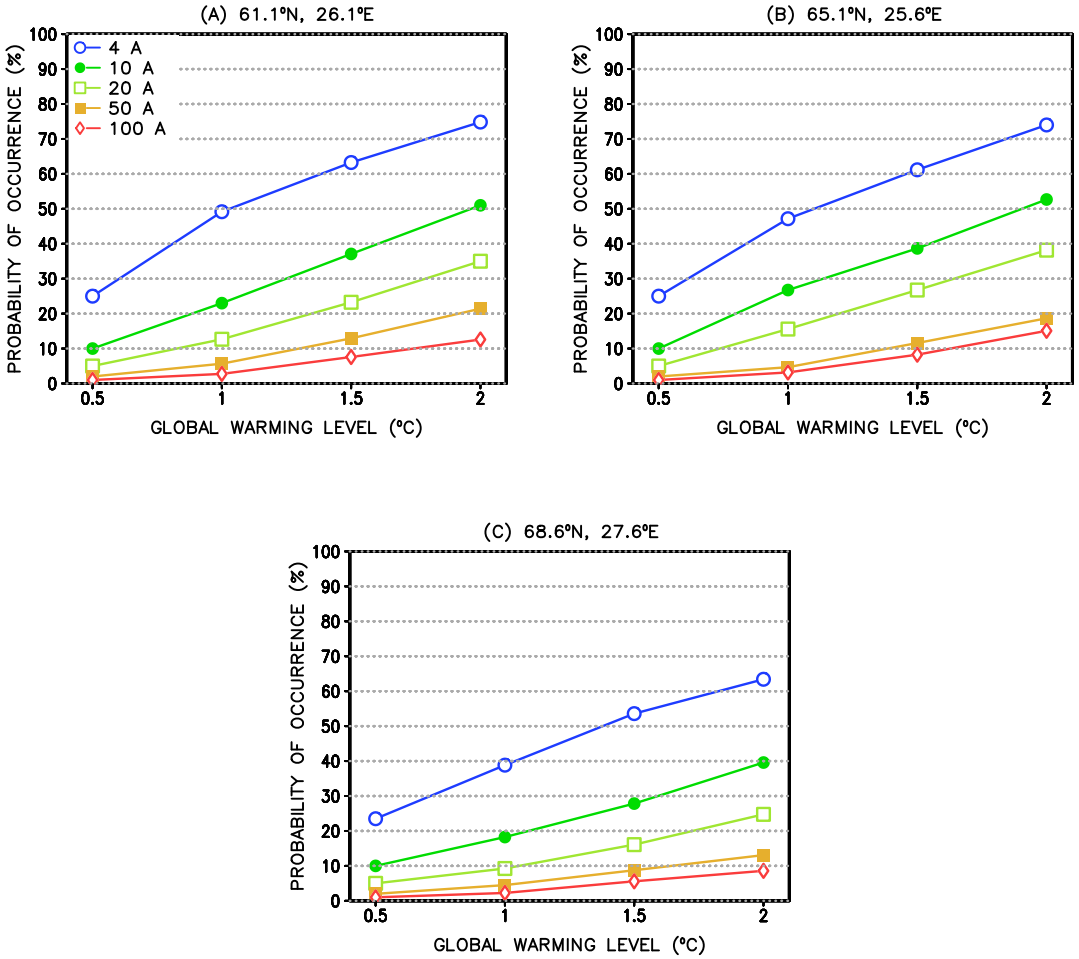

Fig. 4.3: Probabilities (in %) for the occurrence of an annual maximum heatwave (above the 20°C threshold temperature) with the extremity index higher than that occurring once in 4, 10, 20, 50 or 100 years (see the legend in panel (a)) in the baseline climate (0.5 °C global warming) as a function of the level of global warming. The probabilities are shown for three positions: (a) 61.125°N, 26.125°E, (b) 65.125°N, 25.625°E, and (c) 68.625°N, 27.625°E.

paper.

Furthermore, Fig. 4.3 reveals that warming realised by the present has already affected the likelihoods of severe heatwaves considerably. To give some examples, at the 1.0 °C global warming level, the probability of a baseline-period once-in-4-year heatwave has nearly doubled, and 50-year heatwaves have become 2–3 times as likely. Indeed, three of the six major historical heatwaves depicted in Fig. 2.1 have occurred since 2010. Admittedly, within the fairly short observational time span, the occurrence of hot summers is significantly affected by random inter-annual variations in the weather conditions.

In the observed historical climate of Finland, heatwaves with EX $\geq$ 60 °C days can be regarded as extreme. In the south, this limit has been exceeded in a few years, mainly in 2010 and 2018, and in the north only in a small area in 1972 (Fig. 2.1). Table 4.1 shows that warming taken place by the present (the 1.0 °C warming level) has already enhanced the likelihood of such extreme heatwaves substantially, and they are further projected to be much more frequent in the future. In the region of Oulu, for instance, the probability increases 4.5-fold under the 1.5 °C and 12-fold under the 2.0 °C warming level, compared with the 1.0 °C warming level. In the north, heatwaves of that intensity are projected to be fairly rare even at the 2.0 °C global warming. This again emphasises the severity of the heat spell that occurred in Lapland in 1972.

Table 4.1: Annual probabilities (in %) for the occurrence of at least a single heatwave event with the extremity index EX $\geq$ 60 °C days under four levels of global warming (0.5 °C, 1.0 °C, 1.5 °C, and 2.0 °C) at three grid points: 61.125°N, 26.125°E (southern), 65.125°N, 25.625°E (central/Ostrobothnian) and 68.625°N, 27.625°E (northern). The threshold temperature used for a hot day is 20 °C.

Grid point	0.5 °C	1.0 °C	1.5 °C	2.0 °C
Southern	1.1	2.9	8.1	13.5
Central	0.1	0.4	1.8	4.7
Northern	0.1	0.1	0.5	1.5

5 Discussion

5.1 Global warming of 1.5 °C *or* 2.0 °C *– are there pronounced differences?*

The aim of the Paris Agreement on Climate Change was to restrict global warming to either 1.5 °C or 2.0 °C relative to the pre-industrial climate. The present findings indicate that both warming levels entail a substantial strengthening in the average and extreme heatwaves. Nevertheless, in particular when studying the occurrence of the most extreme heatwaves, there is a great jump from the 1.5 °C to the 2.0 °C climate. To provide an example, at the northern (Ivalo) grid point the long-term mean total annual EX above 20 °C increases from 2.6 °C days at the 0.5 °C warming level to 13.4 °C days by the 2.0 °C level (the best estimate or multi-model mean in Table 3.1a), and 42 % of this increase materialises between the 1.5 and 2.0 °C levels. The corresponding proportions for the Ostrobothnian and southern point with the 24 °C threshold temperature are 52 % and 42 %, respectively (Table 3.1b). Accordingly, when we study heatwaves that are severe

relative to the local climate, about a half of the projected total increase in the mean annual heatwave burden is realised between the 1.5 and 2.0 °C global warming levels.

Furthermore, there are major differences in the annual likelihood of occurrence of intense heatwaves between these two warming levels. According to Fig. 4.3a–b, heatwaves occurring once in 50 a at the 0.5 °C warming level have annual probabilities of 12–13 % at the 1.5 °C warming level and 19–21 % at the 2.0 °C level. Thus, the incidence becomes more than 1.6-fold between these two warming levels. Correspondingly, the likelihood of heatwaves with EX $\geq$ 60 °C days approximately triples between the 1.5 °C and 2.0 °C global warming levels at the northernmost points and becomes 1.7-fold at the southern point (Table 4.1).

To conclude, considerable differences in the heatwave characteristics are projected between the 1.5 °C and 2 °C global warming levels, both in the time-mean extremity index and the frequency of severe heatwaves. This disparity is largest for the most extreme heatwave events.

5.2 Factors of uncertainty

The bias correction method applied in this work is fairly simple, adjusting the temporal mean and standard deviation of simulated daily-mean temperatures to be consistent with the observational E-OBS analysis, but ignoring potential biases in the skewness and higher moments of the temperature frequency distribution. If some another bias adjustment method, examples of which are given in *Räisänen and Räty* (2013), for instance, were used, it might have some impact on the findings. Even so, the present correction method involves the great advantage that modelled changes in the mean temperature are not distorted. In any bias-correction method, problems may emerge at those coastal grid points which consist of land in the observational analysis but are treated as sea in some GCMs, or vice versa. This is so because air temperatures tend to vary less intensively in coastal than inland regions.

A trivial source of uncertainty is constituted by inter-model differences and the selection of models. Especially for the very intense heatwaves, differences among the projections produced by the various GCMs tend to be large (Fig. 3.3 and Table 3.1). This may partly be a sampling issue, since very extreme heatwaves are infrequent, and their occurrence is thus strongly affected by stochastic factors. Moreover, the simulated warming of Northern-European summers diverges among the GCMs, despite the use of fixed global warming levels. For example, considering the Ostrobothnian grid point (65.125°N, 25.625°E) examined in Tables 3.1 and 4.1, the 25-GCM mean temperature increase in June-August from the 0.5 to 2.0 °C global warming level is 2.5 °C, while the uncertainty interval defined by the GCMs simulating the second-lowest and second-highest warming is 1.8 to 3.3 °C. Other potential influencing factors are inter-model differences in the shape of the frequency distribution of daily mean temperatures and the temporal autocorrelation of temperature, which affects the clustering of hot days; these two statistical features are not adjusted by the bias correction algorithm. For example, any model deficiencies in describing clusters of hot days due to over- or underestimation of the persistence of high-

pressure systems affect the occurrence of simulated heatwaves.

In Section 2.4 of RJ23, time-mean heatwave indices in the baseline climate derived from the bias-corrected GCM data and the E-OBS analyses were compared with one another, and the compatibility was found to be at least reasonable; this was especially true when looking at the 25-GCM means. This is mainly attributed to the bias correction, which forces the model-simulated climate to match with observations.

For other potential sources of uncertainty in the heatwave projections, the reader is referred to the discussion presented in Section 6.2 of RJ23.

5.3 Implications of heatwaves

Here, some selected impacts of severe heatwaves are mainly discussed from the perspective of Finland and other northern European areas.

In the future, preparedness to respond to heatwaves is becoming increasingly important within social welfare and heat care services (*Curtis et al.*, 2017; *Kollanus et al.*, 2023; *Rapeli and Mussalo-Rauhamaa*, 2022). In particular, prolonged periods with high temperatures cause multiple issues for health. For example, the heatwave experienced in Russia in 2010 killed approximately 55,000 people (*Barriopedro et al.*, 2011). The impacts of heat are felt even in cool climates, elderly population being especially susceptible (*Kollanus et al.*, 2021; *Ruuhela et al.*, 2018, 2017). For example, heatwaves act to increase deaths due to respiratory diseases, renal diseases, mental and behavioural disorders, diseases of the nervous system and cardiovascular diseases, including heart attacks (*Kollanus et al.*, 2021). Heatwaves likewise affect morbidity: a relationship has been found between the heatwaves and hospital admissions due to respiratory diseases, albeit the statistical significance of this connection depends on the age of patients, type of disease and characteristics of the heatwave event (*Sohail et al.*, 2020).

According to *Ruuhela et al.* (2017), additional mortality caused by high temperatures has decreased over the past half century, which suggests that at least in countries with a cool climate, it might be possible to adapt oneself to the increasing heat. On the other hand, urbanization and the accompanied urban heat island (UHI) effect (*Ramamurthy et al.*, 2017) may notably contribute to the heat-related health issues. In the city of Helsinki, modelled mortality attributable to the heatwaves in 2003, 2010, 2014, and 2018 (Fig. 2.1) appeared to be about 2.5 times as large as that in the surrounding rural regions (*Ruuhela et al.*, 2021). A review of UHI studies in Finland did not reveal any notable long-term changes in their intensity (*Drebs et al.*, 2023).

Even in the recent past climate of Finland, approximately corresponding to the global warming level of 1.0 °C, buildings without efficient active or passive cooling system are at a risk of overheating during prolonged heatwaves, and the risk of uncomfortably high indoor temperatures is growing with continuing warming (*Velashjerdi Farahani et al.*, 2021). In buildings equipped with cooling devices, the consumption of cooling energy will increase. Model simulations of the performance of a typical office building indicate that about 50 % extra electricity was consumed for cooling in the very hot summer of 2018, compared with the consumption in the weather conditions of an average current-climate

warm season (*Velashjerdi Farahani et al.*, 2022). In analogous extreme weather conditions around the year 2050, near the anticipated time of the global warming of 2.0 °C, the consumption would further approximately double compared to that in 2018.

In nuclear power plants, heatwaves belong to such external events that have to be taken into consideration in order to ensure an safe and uninterrupted operation of the plants in the changing climate (*Jylhä et al.*, 2018; *Kopytko and Perkins*, 2011; *Unger et al.*, 2021). Unprecedently high air temperatures might endanger a safe shutdown of the plants. Besides, heatwaves tend to warm up seas and the inland watersheds that act as sources of cooling water for the plants. Thus, unusually high water temperatures may force the companies to reduce the nuclear power generation in order to comply with the local environmental water permit conditions; such a situation occurred in Finland in the summers of 2010, 2018, and 2021 (*Fortum*, 2021). As well, elevated water temperatures during heatwave periods have resulted in nuclear power unavailability in Sweden and France, for instance (*Schneider et al.*, 2021).

For boreal forests, high temperature extremes, and particularly droughts that are typically associated with the heatwave events, constitute a severe climate-change induced risk (*Venäläinen et al.*, 2020). Especially, the growth of spruce trees is anticipated to decelerate (*Hayatgheibi et al.*, 2021). Weather conditions favouring wildfires tend to get more severe and frequent (*Backman et al.*, 2021; *Krikken et al.*, 2021).

For spring cereals, a heatwave occurring in early summer in the critical phase of growth, in conjunction with abundant light, can impede the formation of grains and reduce the yield (*Peltonen-Sainio et al.*, 2015, 2016). Both process-based ecophysiological modelling (*Tao et al.*, 2017) and chamber experiments (*Ingvordsen et al.*, 2018) have emphasised the need for developing new cereal varieties that are resilient to future heatwaves in the northern European conditions with lengthening growing seasons and elevated concentrations of carbon dioxide.

In addition to humans and plants, severe heatwaves stress many animals, e.g., dairy cows (*Ahmed et al.*, 2022) and reindeers (*Rasmus et al.*, 2022; *Turunen et al.*, 2016). Heatwave-like temperatures tend to impair the cognitive abilities of bumblebees (*Gérard et al.*, 2022). Increasing water temperatures in the sea (*Goebeler et al.*, 2022) and inland watersheds affect various fish species divergently; e.g., pikeperches benefit (*Lappalainen et al.*, 2009) while cool water fishes such as salmons and trouts suffer (*Clews et al.*, 2010).

Evidently, the examples discussed above will have multiple adverse financial implications. On the other hand, heatwaves, when not too prolonged and intense, can also entail positive impacts, e.g., for summer recreation and tourism in Finland. Because the projected changes in extreme summer temperatures are more pronounced in southern Europe than in the north (RJ23), the relative attractiveness of northern Europe for summer outdoor leisure activities may increase. However, tourists have been found to tolerate even very high temperatures, while rainy weather is decidedly not preferred (*Koutroulis et al.*, 2018, and references therein). Besides, the vulnerability of summer tourism to climate change does not only depend on future climatic conditions but also on the local adaptive capacity of tourism industry.

6 *Concluding remarks*

In this work, heatwave projections for varying levels of global warming have been derived from a large ensemble of GCM simulations. Before carrying out the actual analyses, modelled daily-mean temperature data have been corrected from biases in the monthly means and temporal standard deviation.

The recent climate change, from the 0.5 °C to 1.0 °C global warming level, has already made severe heatwaves in Finland much more frequent. As global warming inevitably continues in the coming decades (*IPCC*, 2021), heatwaves are projected to become even more frequent and severe. Even under a very optimistic scenario, the Earth will warm at least 1.5 °C compared to the pre-industrial era, but this would require very drastic reductions in the emissions of greenhouse gases. Thus, it is necessary to prepare oneself for a 2.0 °C global warming at a minimum. The findings presented in this paper indicate that this would lead to a much more severe heatwave burden than the more stringent 1.5 °C global warming target, also in the cool climate of Finland. For example, the annual likelihood of very intense heatwaves increases by 50–80 %. As summarised in Section 5.3, the projected intense heatwaves would entail severe issues for public health, forestry, fishery, agriculture, reindeer husbandry and many other sectors of society.

Acknowledgments

This work was financed by the following projects of the Academy of Finland: HEATCLIM (decision number 329307), CHAMPS (329225), FINSCAPES (342561), and LEGITIMACY (335562), and by the National Nuclear Waste Management Fund (Dnro SAFER 6/2023 for the MAWECLI project). Computing resources were available from the Centre for Scientific Computing (CSC), Finland. The CMIP6 GCM data were provided by the Earth System Grid Federation (ESGF) data archive (https://esgf-data.dkrz.de/search/cmip6-dkrz/).

References

Aalto, J., I. Lehtonen, P. Pirinen, K. Aapala and R. K. Heikkinen, 2023. Bioclimate change across the protected area network of Finland. *Science of the Total Environment*, **893**, 164782. DOI: 10.1016/j.scitotenv.2023.164782.

Ahmed, H., L.-M. Tamminen and U. Emanuelson, 2022. Temperature, productivity, and heat tolerance: Evidence from Swedish dairy production. *Climatic Change*, **175**, 10. DOI: 10.1007/s10584-022-03461-5.

Backman, L., T. Aalto, I. Lehtonen, L. Thölix, I. Vanha-Majamaa and A. Venäläinen, 2021. "Climate change increases the risk of forest fires". In: *Climate change and forest management affect forest fire risk in Fennoscandia*. Ed. by J. Aalto and A. Venäläinen. Reports 2021:3. Finnish Meteorological Institute, 66–91. URL: http://hdl.handle.net/10138/330898.

Baldwin, J. W., J. B. Dessy, G. A. Vecchi and M. Oppenheimer, 2019. Temporally Compound Heat Wave Events and Global Warming: An Emerging Hazard. *Earth's Future*, **7**, 411–427. DOI: 10.1029/2018EF000989.

Barriopedro, D., E. M. Fischer, J. Luterbacher, R. M. Trigo and R. García-Herrera, 2011. The Hot Summer of 2010: Redrawing the Temperature Record Map of Europe. *Science*, **332**, 220–224. DOI: 10.1126/science.1201224.

Cardell, M. F., A. Amengual, R. Romero and C. Ramis, 2020. Future extremes of temperature and precipitation in Europe derived from a combination of dynamical and statistical approaches. *International Journal of Climatology*, **40**, 4800–4827. DOI: 10.1002/joc.6490.

Clews, E., I. Durance, I. P. Vaughan and S. J. Ormerod, 2010. Juvenile salmonid populations in a temperate river system track synoptic trends in climate. *Global Change Biology*, **16**, 3271–3283. DOI: 10.1111/j.1365-2486.2010.02211.x.

Curtis, S., A. Fair, J. Wistow, D. V. Val and K. Oven, 2017. Impact of extreme weather events and climate change for health and social care systems. *Environmental Health*, **16**, 128. DOI: 10.1186/s12940-017-0324-3.

Drebs, A., J. Suomi and A. Mäkelä, 2023. Urban heat island research at high latitudes — utilising Finland as an example. *Boreal Env. Res.*, **28**, 81–96. URL: https://www.borenv.net/BER/archive/vol%5C_28.html.

Eyring, V., S. Bony, G. A. Meehl, C. A. Senior, B. Stevens, R. J. Stouffer and K. E. Taylor, 2016. Overview of the Coupled Model Intercomparison Project Phase 6 (CMIP6) experimental design and organization. *Geoscientific Model Development*, **9**, 1937–1958. DOI: 10.5194/gmd-9-1937-2016.

Fortum, July 12, 2021. *Loviisan voimalaitoksen ykkösyksikön tehoa lasketaan tilapäisesti meriveden korkean lämpötilan johdosta*. https://www.fortum.fi/media/2021/07/loviisan-voimalaitoksen-ykkosyksikon-tehoa-lasketaan-tilapaisesti-meriveden-korkean-lampotilan-johdosta.

Gérard, M., A. Amiri, B. Cariou and E. Baird, 2022. Short-term exposure to heatwave-like temperatures affects learning and memory in bumblebees. *Global Change Biology*, **28**, 4251–4259. DOI: 10.1111/gcb.16196.

Goebeler, N., A. Norkko and J. Norkko, 2022. Ninety years of coastal monitoring reveals baseline and extreme ocean temperatures are increasing off the Finnish coast. *Communications Earth & Environment*, **3**, 215. DOI: 10.1038/s43247-022-00545-z.

Hausfather, Z., K. Marvel, G. A. Schmidt, J. W. Nielsen-Gammon and M. Zelinka, 2022. Climate simulations: recognize the 'hot model' problem. *Nature*, **605**, 26–29. DOI: 10.1038/d41586-022-01192-2.

Hayatgheibi, H., M. Haapanen, J. Lundströmer, M. Berlin, K. Kärkkäinen and A. Helmersson, 2021. The Impact of Drought Stress on the Height Growth of Young Norway Spruce Full-Sib and Half-Sib Clonal Trials in Sweden and Finland. *Forests*, **12**, 498. DOI: 10.3390/f12040498.

Haylock, M. R., N. Hofstra, A. M. G. Klein Tank, E. J. Klok, P. D. Jones and M. New, 2008. A European daily high-resolution gridded dataset of surface temperature and

precipitation for 1950–2006. *J. Geophys. Res.*, **113** (D20), D20119. DOI: 10.1029/2008JD010201.

Hutila, A., 2010. Heinäkuun 2010 helteet poikkeuksellisia. *Ilmastokatsaus*, **2010**, 7. URL: https://www.ilmastokatsaus.fi/wp-content/uploads/2021/04/2010%5C_07%5C_heinakuu.pdf.

Ingvordsen, C. H., M. F. Lyngkjær, P. Peltonen-Sainio, T. N. Mikkelsen, A. Stockmarr and R. B. Jørgensen, 2018. How a 10-day heatwave impacts barley grain yield when superimposed onto future levels of temperature and CO_2 as single and combined factors. *Agriculture, Ecosystems & Environment*, **259**, 45–52. DOI: 10.1016/j.agee.2018.01.025.

IPCC, 2021. *Climate Change 2021: The Physical Science Basis. Contribution of Working Group I to the Sixth Assessment Report of the Intergovernmental Panel on Climate Change*. [Masson-Delmotte, V., P. Zhai, A. Pirani, S.L. Connors, C. Péan, S. Berger, N. Caud, Y. Chen, L. Goldfarb, M.I. Gomis, M. Huang, K. Leitzell, E. Lonnoy, J.B.R. Matthews, T.K. Maycock, T. Waterfield, O. Yelekci, R. Yu and B. Zhou (eds.)] Cambridge, U.K., 2391 pp: Cambridge University Press.

Jylhä, K., M. Kämäräinen, C. Fortelius, H. Gregow, J. Helander, O. Hyvärinen, M. Johansson, A. Karppinen, A. Korpinen, R. Kouznetsov, E. Kurzeneva, U. Leijala, A. Mäkelä, H. Pellikka, S. Saku, J. Sandberg, M. Sofiev, A. Vajda, A. Venäläinen and J. Vira, 2018. Recent meteorological and marine studies to support nuclear power plant safety in Finland. *Energy*, **165**, 1102–1118. DOI: 10.1016/j.energy.2018.09.033.

Kim, S., V. A. Sinclair, J. Räisänen and R. Ruuhela, 2018. Heat waves in Finland: present and projected summertime extreme temperatures and their associated circulation patterns. *International Journal of Climatology*, **38**, 1393–1408. DOI: 10.1002/joc.5253.

Kollanus, V., J. I. Halonen and T. Lanki, 2023. Helteen vaikutukset ja varautuminen terveydenhuollossa. *Duodecim*, **139**, 1127–1133.

Kollanus, V., P. Tiittanen and T. Lanki, 2021. Mortality risk related to heatwaves in Finland —Factors affecting vulnerability. *Environmental Research*, **201**, 111503. DOI: 10.1016/j.envres.2021.111503.

Kopytko, N. and J. Perkins, 2011. Climate change, nuclear power, and the adaptation-mitigation dilemma. *Energy Policy*, **39**, 318–333. DOI: 10.1016/j.enpol.2010.09.046.

Koutroulis, A. G., M. G. Grillakis, I. K. Tsanis and D. Jacob, 2018. Mapping the vulnerability of European summer tourism under 2 C global warming. *Climatic Change*, **151**, 157–171. DOI: 10.1007/s10584-018-2298-8.

Krikken, F., F. Lehner, K. Haustein, I. Drobyshev and G. J. van Oldenborgh, 2021. Attribution of the role of climate change in the forest fires in Sweden 2018. *Natural Hazards and Earth System Sciences*, **21**, 2169–2179. DOI: 10.5194/nhess-21-2169-2021.

Kyselý, J., 2010. Recent severe heat waves in central Europe: How to view them in a long-term prospect? *International Journal of Climatology*, **30**, 89–109. DOI: 10.1002/joc.1874.

Lappalainen, J., M. Milardi, K. Nyberg and A. Venäläinen, 2009. Effects of water temperature on year-class strengths and growth patterns of pikeperch [Sander lucioperca (L.)] in the brackish Baltic Sea. *Aquatic Ecology*, **43**, 181–191. DOI: 10.1007/s10452-007-9150-y.

Lhotka, O., J. Kyselý and A. Farda, 2018. Climate change scenarios of heat waves in Central Europe and their uncertainties. *Theor Appl Climatol*, **131**, 1043–1054. DOI: 10.1007/s00704-016-2031-3.

Näyhä, S., 2005. Environmental temperature and mortality. *International Journal of Circumpolar Health*, **64**, 451–458.

O'Neill, B. C., C. Tebaldi, D. P. van Vuuren, V. Eyring, P. Friedlingstein, G. Hurtt, R. Knutti, E. Kriegler, J.-F. Lamarque, J. Lowe, G. A. Meehl, R. Moss, K. Riahi and B. M. Sanderson, 2016. The Scenario Model Intercomparison Project (ScenarioMIP) for CMIP6. *Geoscientific Model Development*, **9**, 3461–3482. DOI: 10.5194/gmd-9-3461-2016.

Otto, F. E. L., N. Massey, G. J. van Oldenborgh, R. G. Jones and M. R. Allen, 2012. Reconciling two approaches to attribution of the 2010 Russian heat wave. *Geophysical Research Letters*, **39**. DOI: 10.1029/2011GL050422.

Ouzeau, G., J.-M. Soubeyroux, M. Schneider, R. Vautard and S. Planton, 2016. Heat waves analysis over France in present and future climate: Application of a new method on the EURO-CORDEX ensemble. *Climate Services*, **4**, 1–12. DOI: 10.1016/j.cliser.2016.09.002.

Peltonen-Sainio, P., L. Jauhiainen, T. Palosuo, K. Hakala and K. Ruosteenoja, 2015. Rainfed crop production challenges under European high-latitude conditions. *Regional Environmental Change*. DOI: 10.1007/s10113-015-0875-1.

Peltonen-Sainio, P., P. Pirinen, H. M. Mäkelä, O. Hyvärinen, E. Huusela-Veistola, H. Ojanen and A. Venäläinen, 2016. Spatial and temporal variation in weather events critical for boreal agriculture: I Elevated temperatures. *Agricultural and Food Science*, **25**, 44–56. DOI: 10.23986/afsci.51465.

Räisänen, J. and O. Räty, 2013. Projections of daily mean temperature variability in the future: cross-validation tests with ENSEMBLES regional climate simulations. *Clim Dyn*, **41**, 1553–1568. DOI: 10.1007/s00382-012-1515-9.

Ramamurthy, P., J. González, L. Ortiz, M. Arend and F. Moshary, 2017. Impact of heatwave on a megacity: an observational analysis of New York City during July 2016. *Environmental Research Letters*, **12**, 054011. DOI: 10.1088/1748-9326/aa6e59.

Rantanen, M., K. Ruosteenoja, S. Luhtala, M. Virman, H. Pellikka, S. Polade, R. Ruuhela and A. Luomaranta, 2023. Ilmastonmuutos pääkaupunkiseudulla. Raportteja 2023:1. In Finnish with abstract in English and Swedish. Ilmatieteen laitos, 35. DOI: 10.35614/isbn.9789523361737.

Rapeli, M. and H. Mussalo-Rauhamaa, 2022. Intensive and residential elderly care services responding to heat wave — case Finland. *Nordic Social Work Research*, 1–12. DOI: 10.1080/2156857X.2022.2047767.

Rasmus, S., T. Horstkotte, M. Turunen, M. Landauer, A. Löf, I. Lehtonen, G. Rosqvist and Ø. Holand, 2022. "Reindeer husbandry and climate change: challenges for adaptation". In: *Reindeer husbandry and global environmental change: Pastoralism in Fennoscandia*. Ed. by T. Horstkotte, Ø. Holand, J. Kumpula and J. Moen. Routledge, 99–117. DOI: 10.4324/9781003118565-8.

Ruosteenoja, K., 2021. Applicability of CMIP6 models for building climate projections for northern Europe. Reports 2021:7. Finnish Meteorological Institute, 48. DOI: 10.35614/isbn.9789523361416.

Ruosteenoja, K. and K. Jylhä, 2021. Projected climate change in Finland during the 21st century calculated from CMIP6 model simulations. *Geophysica*, **56**, 39–69.

Ruosteenoja, K. and K. Jylhä, 2023. Average and extreme heatwaves in Europe at 0.5-2.0 C global warming levels in CMIP6 model simulations. *Climate Dynamics*, **61**, 4259–4281. DOI: 10.1007/s00382-023-06798-4.

Ruosteenoja, K., J. Räisänen, K. Jylhä, H. Mäkelä, I. Lehtonen, H. Simola, A. Luomaranta and S. Weiher, 2013. Maailmanlaajuisiin CMIP3-malleihin perustuvia arvioita Suomen tulevasta ilmastossa (Climate change estimates for Finland on the basis of global CMIP3 climate models). Raportteja 2013:4. (In Finnish with abstract in English and Swedish). Ilmatieteen laitos, 83.

Ruosteenoja, K., J. Räisänen, A. Venäläinen and M. Kämäräinen, 2016. Projections for the duration and degree days of the thermal growing season in Europe derived from CMIP5 model output. *International Journal of Climatology*, **36**, 3039–3055. DOI: 10.1002/joc.4535.

Ruuhela, R., O. Hyvärinen and K. Jylhä, 2018. Regional Assessment of Temperature-Related Mortality in Finland. *International Journal of Environmental Research and Public Health*, **15**, 406. DOI: 10.3390/ijerph15030406.

Ruuhela, R., K. Jylhä, T. Lanki, P. Tiittanen and A. Matzarakis, 2017. Biometeorological Assessment of Mortality Related to Extreme Temperatures in Helsinki Region, Finland, 1972–2014. *International Journal of Environmental Research and Public Health*, **14**, 944. DOI: 10.3390/ijerph14080944.

Ruuhela, R., A. Votsis, J. Kukkonen, K. Jylh, S. Kankaanp and A. Perrels, 2021. Temperature-Related Mortality in Helsinki Compared to Its Surrounding Region Over Two Decades, with Special Emphasis on Intensive Heatwaves. *Atmosphere*, **12**, 46. DOI: 10.3390/atmos12010046.

Sambou, M.-J. G., B. Pohl, S. Janicot, A. M. s. Landry Famien, P. Roucou, D. Badiane and A. T. Gaye, 2021. Heat waves in spring from Senegal to Sahel: Evolution under climate change. *International Journal of Climatology*, **41**, 6238–6253. DOI: 10.1002/joc.7176.

Schneider, M., A. Froggatt, J. Hazemann, A. Ahmad, M. Budjeryn, Y. Kaido, N. Kan, T. Katsuta, T. Laconde, M. Le Moal, H. Sakiyama, T. Suzuki, M. Ramana, B. Wealer, A. Stienne and F. Meinass, 2021. The World Nuclear Industry Status Report 2021. Tech. rep. France. URL: https://www.worldnuclearreport.org/IMG/pdf/wnisr2021-lr.pdf.

Seneviratne, S., X. Zhang, M. Adnan, W. Badi, C. Dereczynski, A. Di Luca, S. Ghosh, I. Iskandar, J. Kossin, S. Lewis, F. Otto, I. Pinto, M. Satoh, S. Vicente-Serrano, M. Wehner and B. Zhou, 2021. "Weather and Climate Extreme Events in a Changing Climate". In: *Climate Change 2021: The Physical Science Basis. Contribution of Working Group I to the Sixth Assessment Report of the Intergovernmental Panel on Climate Change*. Ed. by V. Masson-Delmotte, P. Zhai, A. Pirani, S. Connors, C. P. an, S. Berger, N. Caud, Y. Chen, L. Goldfarb, M. Gomis, M. Huang, K. Leitzell, E. Lonnoy, J. Matthews, T. Maycock, T. Waterfield, O. Y. i, R. Yu and B. Zhou. Cambridge University Press, Cambridge, United Kingdom. Chap. 11, 1513–1766. DOI: 10.1017/9781009157896.013.

Sohail, H., V. Kollanus, P. Tiittanen, A. Schneider and T. Lanki, 2020. Heat, Heatwaves and Cardiorespiratory Hospital Admissions in Helsinki, Finland. *International Journal of Environmental Research and Public Health*, **17**, 7892. DOI: 10.3390/ijerph17217892.

Tao, F., R. P. Rötter, T. Palosuo, C. Díaz-Ambrona, M. I. Mínguez, M. A. Semenov, K. C. Kersebaum, C. Nendel, D. Cammarano, H. Hoffmann, F. Ewert, A. Dambreville, P. Martre, L. Rodríguez, M. Ruiz-Ramos, T. Gaiser, J. G. Höhn, T. Salo, R. Ferrise, M. Bindi and A. H. Schulman, 2017. Designing future barley ideotypes using a crop model ensemble. *European Journal of Agronomy*, **82**, 144–162. DOI: 10.1016/j.eja.2016.10.012.

Tomczyk, A. M. and E. Bednorz, 2019. Heat waves in Central Europe and tropospheric anomalies of temperature and geopotential heights. *International Journal of Climatology*, **39**, 4189–4205. DOI: 10.1002/joc.6067.

Turunen, M., S. Rasmus, M. Bavay, K. Ruosteenoja and J. Heiskanen, 2016. Coping with difficult weather and snow conditions: Reindeer herders' views on climate change impacts and coping strategies. *Climate Risk Management*, **11**, 15–36. DOI: 10.1016/j.crm.2016.01.002.

Unger, T., E. Kjellström, J. Gode and G. Strandberg, 2021. The impact of climate change on nuclear power. Tech. rep. 2021:744. Energiforsk. URL: https://energiforsk.se/media/29744/the-impact-of-climate-change-on-nuclear-power-energiforskrapport-2021-744.pdf.

Velashjerdi Farahani, A., J. Jokisalo, N. Korhonen, K. Jylhä, R. Kosonen and S. Lestinen, 2022. Performance assessment of ventilative and radiant cooling systems in office buildings during extreme weather conditions under a changing climate. *Journal of Building Engineering*, **57**, 104951. DOI: 10.1016/j.jobe.2022.104951.

Velashjerdi Farahani, A., J. Jokisalo, N. Korhonen, K. Jylhä, K. Ruosteenoja and R. Kosonen, 2021. Overheating Risk and Energy Demand of Nordic Old and New Apartment Buildings during Average and Extreme Weather Conditions under a Changing Climate. *Applied Sciences*, **11**, 3972. DOI: 10.3390/app11093972.

Venäläinen, A., I. Lehtonen, M. Laapas, K. Ruosteenoja, O.-P. Tikkanen, H. Viiri, V.-P. Ikonen and H. Peltola, 2020. Climate change induces multiple risks to boreal forests

and forestry in Finland: A literature review. *Global Change Biology*, **26**, 4178–4196. DOI: 10.1111/gcb.15183.

Wang, G., Q. Zhang, M. Luo, V. P. Singh and C.-Y. Xu, 2022. Fractional contribution of global warming and regional urbanization to intensifying regional heatwaves across Eurasia. *Climate Dynamics*, **59**, 1521–1537. DOI: 10.1007/s00382-021-06054-7.

Zhu, J., S. Wang and E. M. Fischer, 2022. Increased occurrence of day–night hot extremes in a warming climate. *Climate Dynamics*, **59**, 1297–1307. DOI: 10.1007/s00382-021-06038-7.